Spectral statistics, nonequilibrium dynamics, and thermalization in random matrices with global $\mathbb{Z}_2$ symmetry

Adway Kumar Das
School of Science, Loughborough University, Loughborough, Leicestershire LE11 3TU, United Kingdom

(Received 7 January 2026; revised 25 February 2026; accepted 13 March 2026; published 2 April 2026)

$\mathbb{Z}_2$ symmetry is ubiquitous in quantum mechanics, where it drives various phase transitions and emergent physics. The role of $\mathbb{Z}_2$ symmetry in the thermalization of a local observable in a disordered system can be understood using random matrix theory. To do so, we consider random symmetric centrosymmetric (SC) matrix as a toy model where a $\mathbb{Z}_2$ symmetry, namely, the exchange symmetry, is conserved. Such a conservation law splits the Hilbert space into decoupled subspaces such that the energy spectrum of an SC matrix is a superposition of two pure spectra. After discussing the known results on the correlations of such mixed spectra, we consider different initial states and analytically compute the time evolution of their survival probability and associated timescales. We show that there exist certain low-energy initial states which do not decay over a very long timescales such that a measure zero fraction of random SC matrices exhibit spontaneous symmetry breaking. Later, we look at the equilibrium values of local observables like the density-density correlation, kinetic energy operator, and compare them against the average values from the microcanonical and canonical ensembles. We find that when the observable violates (respects) the global symmetry of the Hamiltonian, the equilibrium value is independent (dependent) of the symmetry of the initial state. However, irrespective of such symmetry constraints, the fluctuations of the diagonal terms of the observables within microcanonical shells decay with system size such that the ansatz of the eigenstate thermalization hypothesis remains valid. We show that the equilibrium value converges to the canonical average for all the observables and initial states, indicating that thermalization occurs despite the presence of a global symmetry.

DOI: 10.1103/8v6c-qydj

I. INTRODUCTION

The emergence of statistical mechanics upon equilibration of an isolated quantum system is a fascinating area of research. Despite the unitarity of the time evolution of an isolated system, a typical local observable thermalizes if the energy states of the governing Hamiltonian are ergodic [1] with a correlated energy spectrum [2–6]. Surprisingly, many strongly correlated interacting many-body systems violate thermalization due to breaking of ergodicity [7–10], measure zero athermal initial states, i.e., quantum scars [11–14], kinetic constraints in glassy systems [15–18], and emergent integrals of motion from many-body localization [19–21]. Violation of thermalization is also observed in single-particle systems [22], where approximately conserved charges can form due to on-site disorder or inhomogeneous hopping terms [23–27]. Thus, it is important to understand the role of conservation laws, hence, the underlying symmetries of a system in the statistical description of its equilibrium properties.

In a two-level system, the presence of a single nontrivial symmetry ensures integrability, where the energy levels become uncorrelated with localized eigenstates [28–30]. This naturally leads to the question of what happens in a disordered system with many degrees of freedom upon breaking a single global symmetry [31,32]. In this work, we focus on the discrete $\mathbb{Z}_2$ symmetry where the Hamiltonian commutes with an invertible symmetry operator $\hat{\mathsf{O}}$ possessing only two distinct nonzero eigenvalues. $\mathbb{Z}_2$ symmetry is ubiquitous in physics, i.e., spontaneous breaking of a $\mathbb{Z}_2$ symmetry leads to quantum phase transition in transverse field Ising [33], coupled top [34,35], Lipkin-Meshkov-Glick [36,37], and Dicke [38–40] models. The degenerate spectrum of $\hat{\mathsf{O}}$ implies that an N-dimensional Hilbert space with $N \gg 1$ can be split into two decoupled subspaces labeled by two different good quantum numbers. Consequently, any excitation initially localized on a particular subspace will always be restricted there if the governing Hamiltonian commutes with the symmetry operator $\hat{\mathsf{O}}$.

If the symmetry imposed by $\hat{\mathsf{O}}$ is slightly perturbed, the initially decoupled subspaces get weakly coupled. Then, starting from one subspace, a localized excitation can leak to the complementary subspace with a finite probability. This leads to the thermalization of a generic local observable at sufficiently long times. But, within some intermediate time window, the nonequilibrium dynamics may exhibit long-lived metastable states, known as prethermalization [10,41–45]. This has important ramifications in various problems, e.g., breaking parity in nuclear physics [46], isospin mixing [47–49], and exciton transfer [50–52]. Such explicit symmetry breaking not only affects the properties of quantum mechanical but also of classical systems as well, e.g., acoustic resonances in

Published by the American Physical Society under the terms of the Creative Commons Attribution 4.0 International license. Further distribution of this work must maintain attribution to the author(s) and the published article's title, journal citation, and DOI.

anisotropic quartz block [53–55], small-world [56], biological [57] networks. Other than breaking symmetry, weakly coupled subspaces can also form due to emergent phenomena, e.g., quantum Zeno effect [58], cooperative shielding due to long-range interactions [59].

As a concrete example of $\mathbb{Z}_2$ symmetry in a disordered system, we consider the random symmetric centrosymmetric (SC) matrices, which commute with the exchange symmetry operator J. Such a discrete symmetry is important in diverse disciplines ranging from information theory [60,61] to engineering problems [62,63]. In the construction of a pre-engineered quantum wire (i.e., a network of qubits), exchange symmetry is shown to play a central role to ensure perfect transfer of information between the input and output qubits [64–69]. The exchange symmetry is also important for the transfer fidelity in the photosynthetic structures [50,51] and disordered networks [31,52].

In this work, we take random SC matrices and look at the dynamics of various initial states that are either confined to a particular symmetry sector or couple the symmetry sectors with a tunable parameter. In case of such initial states, we look at the equilibrium values of various local observables and compare them with the predictions from different statistical ensembles. Our system size-scaling analyses indicate that thermalization occurs in the case of a generic observable despite the presence of a global symmetry, and the equilibrium value is described by the Gibbs ensemble [9,45,70–72].

The organization of the paper is as follows: in Sec. II, we define the exchange symmetry, SC matrices, and discuss some of their general properties. In Sec. II A, we provide the analytical expressions of the energy correlations in the case of a random SC matrix. In Sec. III, we show the analytical expression of the survival probability of certain initial states and discuss the characteristic timescales. Importantly, we show that spontaneous symmetry breaking can happen in a measure-zero fraction of the random SC matrices. In Sec. IV, we discuss the general notion of thermalization in an isolated system and the equilibration of various observables with respect to different initial states in the case of the SC matrices. Our concluding remarks are given in Sec. V.

II. SYMMETRIC CENTROSYMMETRIC MATRIX

An $N \times N$ centrosymmetric matrix H satisfies the commutation relation

$$[H, \mathsf{J}] = 0 \Rightarrow H_{i,j} = H_{i',j'} \;\forall\; i, j, \quad i' \equiv N + 1 - i, \tag{1}$$

where the exchange matrix $\mathsf{J} \equiv \{\delta_{i,N+1-j}\}$ is symmetric, invertible ($\mathsf{J} = \mathsf{J}^{-1} = \mathsf{J}^T$), involutory ($\mathsf{J}^2 = \mathbb{I}$, the identity matrix), and has two distinct eigenvalues ± 1 with multiplicities $\lceil \frac{N}{2} \rceil$ and $\lfloor \frac{N}{2} \rfloor$, respectively. If $N = 2^L$, an $N \times N$ exchange matrix can be expressed as $\bigotimes_k \sigma_k^x$ where σ_k^x is the Pauli X matrix in $\hat{\sigma}_z$ representation acting on the kth site of a fictitious one-dimensional (1D) lattice with L sites. Since $[\sigma^x, \mathbb{I}] = 0$, any matrix of the form $\sigma_i^x \sigma_j^x \cdots \sigma_k^x$ commutes with J where $1 \leqslant i < \cdots < k \leqslant L$. The exchange matrix also commutes with the matrices of the form

$$\mathbb{I}^{N_1 \times N_1} \oplus \mathsf{O} \oplus \mathbb{I}^{N_2 \times N_2} \oplus \mathsf{JOJ} \oplus \mathbb{I}^{N_1 \times N_1}, \tag{2}$$

where O is any arbitrary operator of dimension $N - (2N_1 + N_2)$.

A matrix H with both centrosymmetry and diagonal symmetry is called symmetric centrosymmetric (SC),

$$H = \mathsf{J}H^T\mathsf{J} \Leftrightarrow H_{i,j} = H_{j',i'}, \tag{3}$$

which is persymmetric as well [73]. Since $[H, \mathsf{J}] = 0$, we can reduce H in the basis of J via a similarity transformation $Q^T H Q = H'$ such that H' assumes a block-diagonal form. Such a block structure is a consequence of the two disjoint subspaces in the Hilbert space, which are denoted by odd and even sectors, spanned by antisymmetric ($|\Phi^-\rangle$) and symmetric ($|\Phi^+\rangle$) states with energy levels $E^{\mp}$, respectively [31].

Energy correlations of an SC matrix

We look at random SC matrices having independent and identically distributed Gaussian random elements with zero mean and unit variance. The corresponding energy spectrum is a superposition of two pure spectra, each belonging to a Gaussian orthogonal ensemble (GOE) matrix. The energy correlations in the case of such a mixed spectrum are well known [74]. Below, we provide the analytical forms of the energy correlations for a random SC matrix for the sake of completeness.

The density of states of a random SC matrix follows Wigner's semicircle law with a width $2(\langle E^2 \rangle)^{1/2} = \sqrt{4+N}$. Corresponding energy levels exhibit level clustering with the density of level spacing [74,75]

$$\mathrm{P}^{\mathrm{SC}}(s) = \frac{e^{-\frac{\pi}{8}s^2}}{2} + \frac{\pi}{8} s e^{-\frac{\pi}{16}s^2} \mathrm{Erfc}\left(\frac{\sqrt{\pi}}{4} s\right), \tag{4}$$

and the second moment of the level spacing is

$$\langle s^2 \rangle = \frac{8(2-\sqrt{2})}{\pi}. \tag{5}$$

In Fig. 1(a), we plot the numerically obtained density of level spacing of the SC ensemble for $N = 2048$ along with the analytical expression from Eq. (4). The above equation indicates a degree of level repulsion intermediate between that of the GOE and Poisson ensemble ($\langle s^2 \rangle = \frac{4}{\pi}$ and 2 for Wigner's surmise and exponential distribution, respectively). An intermediate level repulsion caused by incomplete separation of symmetries is observed in many-body systems as well [76].

The superposition of two pure spectra also affects the long-range energy correlation of an SC matrix, reflected in the two-point correlation function,

$$\rho^{(2)}(E_1, E_2) = N(N-1) \int dE_3 \cdots dE_N \mathrm{P}(\vec{E}). \tag{6}$$

The above integral relation is valid provided the joint density of the N energy levels, $\mathrm{P}(\vec{E})$ is invariant under the exchange of any pair of energies. The two-point correlation $\rho^{(2)}(E_1, E_2)$ is the probability of finding any two energy levels at E_1 and E_2 [77]. A related quantity is the two-level cluster function $T_2(E) \equiv 1 - \rho^{(2)}(E)$, where $E = E_1 - E_2$.

To understand the universal features of the energy correlations, it is important to unfold the energy spectrum, $\mathcal{E}_j = N\varrho(E_j)$, where $\varrho(x)$ is the cumulative distribution of energy [78]. Unfolding gets rid of the system-dependent global shape

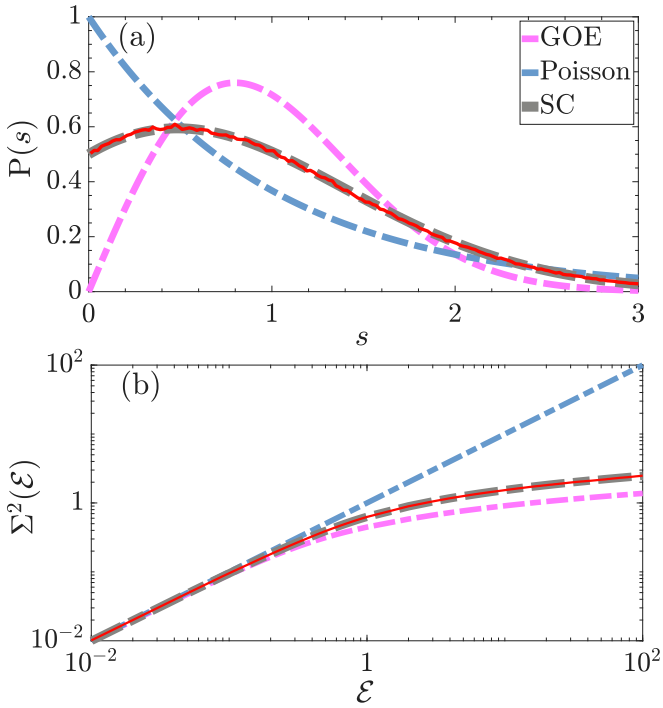


FIG. 1. Energy correlation of random SC matrices: (a) density of level spacing, (b) number variance for $N = 2048$. The solid curves denote numerical results while the dashed lines denote the analytical expressions for Poisson, GOE, and random SC matrices [Eqs. (4) and (13)].

of the density of states and reduces the mean level spacing to unity. We denote the two-level cluster function of the unfolded energy levels as $Y_2(\mathcal{E})$ where $\mathcal{E}$ is the gap of unfolded energy levels. In the Poisson ensemble, $Y_2(\mathcal{E}) = 0$ at any energy gap, while for GOE [75]

$$Y_2^{\mathrm{GOE}}(\mathcal{E}) = \left(\frac{\pi}{2}\mathrm{sgn}(\mathcal{E}) - \mathrm{Si}(\pi\mathcal{E})\right)\left(\frac{\cos\pi\mathcal{E}}{\pi\mathcal{E}} - \frac{\sin\pi\mathcal{E}}{(\pi\mathcal{E})^2}\right) + \left(\frac{\sin\pi\mathcal{E}}{\pi\mathcal{E}}\right)^2, \tag{7}$$

where $\mathrm{sgn}(x)$ is the Signum function and $\mathrm{Si}(x) \equiv \int_0^x dt\,\frac{\sin t}{t}$ is the sine integral. In the case of an SC matrix, the superposition of two GOE spectra leads to a two-level cluster function [74]

$$Y_2^{\mathrm{SC}}(\mathcal{E}) = \frac{1}{2}Y_2^{\mathrm{GOE}}\left(\frac{\mathcal{E}}{2}\right). \tag{8}$$

The inverse Fourier transform of the two-level cluster function gives the two-level form factor, a function in the dimensionless time domain τ,

$$b_2(\tau) = \int_{-\infty}^{\infty} d\mathcal{E}\, Y_2(\mathcal{E})\cos(2\pi\tau\mathcal{E}), \tag{9}$$

where the symmetry of $Y_2(\mathcal{E})$ around $\mathcal{E} = 0$ reduces the complex integral to a real one [79]. The two-level form factor controls the long-time dynamics of a generic observable [80]. For the Poisson ensemble, $b_2(\tau) = 0$ at any time, while for GOE

$$b_2^{\mathrm{GOE}}(\tau) = \begin{cases} 1 - 2\tau + \tau\ln(1+2\tau), & \tau \leqslant 1 \\ \tau\ln\left(\dfrac{2\tau+1}{2\tau-1}\right) - 1, & \tau > 1. \end{cases} \tag{10}$$

Then, Eq. (8) implies that the two-level form factor of an SC matrix is $b_2^{\mathrm{SC}}(\tau) = b_2^{\mathrm{GOE}}(2\tau)$.

To identify different energy scales in a system, one of the most useful measures is the number variance, defined for a set of unfolded energies, $\{\mathcal{E}_j\}$ as [81],

$$\Sigma^2(\mathcal{E}) = \langle[\mathcal{N}(\mathcal{E},\mathcal{E}_0) - \mathcal{E}]^2\rangle_{\mathcal{E}_0},$$
$$\mathcal{N}(\mathcal{E},\mathcal{E}_0) = I\left(\mathcal{E}_0 + \frac{\mathcal{E}}{2}\right) - I\left(\mathcal{E}_0 - \frac{\mathcal{E}}{2}\right), \tag{11}$$

where $I(\mathcal{E})$ is the cumulative distribution of the unfolded energy levels, and $\mathcal{N}(\mathcal{E},\mathcal{E}_0)$ is the number of energy levels in the window of span $\mathcal{E}$ and centered at $\mathcal{E}_0$. For GOE, the energy spectrum is rigid so that any two energy levels are correlated, and the number variance has a logarithmic behavior [75,82],

$$\Sigma^2_{\mathrm{GOE}}(\mathcal{E}) = \frac{2}{\pi^2}\ln\left(2\pi\mathcal{E} + \gamma_{\mathrm{E}} + 1 - \frac{\pi^2}{8}\right) + O\left(\frac{1}{\mathcal{E}}\right), \tag{12}$$

where $\gamma_{\mathrm{E}} = 0.577216\ldots$ is the Euler-Mascheroni constant, $\mathrm{Ci}(x) = -\int_x^\infty dt\,\frac{\cos t}{t}$ and $\mathrm{Si}(x) = \int_0^x dt\,\frac{\sin t}{t}$. Contrarily, in the Poisson ensemble, the number of unfolded energy levels is free to fluctuate around their mean position, $\langle\mathcal{N}(\mathcal{E},\mathcal{E}_0)\rangle_{\mathcal{E}_0} = \mathcal{E}$ and the number variance exhibits a linear behavior, $\Sigma^2(\mathcal{E}) = \mathcal{E}$. In the case of an SC matrix, superposition implies that the number variance follows [74]

$$\Sigma^2_{\mathrm{SC}}(\mathcal{E}) = 2\Sigma^2_{\mathrm{GOE}}\left(\frac{\mathcal{E}}{2}\right). \tag{13}$$

In Fig. 1(b), we plot the numerically obtained number variance of SC ensemble for $N = 2048$ along with the analytical expression from Eq. (13) and find an excellent agreement. Thus, we have closed-form analytical expressions of both the short- and long-range energy correlations of the SC matrices.

III. DYNAMICAL RESPONSE OF AN SC MATRIX

The exchange symmetry of an SC matrix implies that the dynamics of an initial state will depend on its symmetry. To illustrate this, we look at the following initial state:

$$|\Psi_\omega\rangle \equiv \cos\omega|k\rangle + \sin\omega|k'\rangle, \quad -\frac{\pi}{2} \leqslant \omega \leqslant \frac{\pi}{2}, \tag{14}$$

where $k' \equiv N + 1 - k$ and $|k\rangle$ is any unit vector from the computational basis. The expectation value of the exchange symmetry with respect to $|\Psi_\omega\rangle$ is

$$\langle\mathsf{J}\rangle = \langle\Psi_\omega|\mathsf{J}|\Psi_\omega\rangle = \sin(2\omega). \tag{15}$$

Our choice of the initial state is motivated by Schrödinger's cat states, which are superpositions of macroscopically different states [83–86]. In particular, $|\Psi_\omega\rangle$ is a weighted superposition of the exchange doublets, $(|k\rangle \pm |k'\rangle)/\sqrt{2} \equiv |\Psi_{\pm\frac{\pi}{4}}\rangle$, which are eigenstates of J and have energies $H_{k,k} \pm H_{k,k'}$ with respect to the Hamiltonian H.

The local density of states [80,87–90] of $|\Psi_\omega\rangle$ is

$$\rho_\omega(E) = \sum_{j=\pm}\sum_{n=1}^{\frac{N}{2}} |c_n^j|^2 \delta\left(E - E_n^j\right),$$
$$c_n^\pm \equiv \langle \Phi_n^\pm | \Psi_\omega\rangle = (\cos\omega \pm \sin\omega)\Phi_n^\pm(k), \tag{16}$$

where $|\Phi_n^\pm\rangle$ are eigenstates of H with energies $E_n^\pm$. In case of the SC matrices, $\rho_\omega(E)$ follows Wigner's semicircle law with a width $\Gamma \approx \frac{\sqrt{N}}{2}$, irrespective of ω. However, for $\omega = \frac{\pi}{4}$, $|\Psi_\omega\rangle$ is a symmetric state (having $\langle \mathrm{J}\rangle = 1$), hence, spanned by only $|\Phi_j^+\rangle$'s, the symmetric eigenstates of H. Consequently, the time evolution of $|\Psi_\omega\rangle$ is always confined to the even subspace. Similarly, the time evolution of $|\Psi_{-\frac{\pi}{4}}\rangle$ is always restricted to the odd subspace spanned by antisymmetric energy eigenstates, $|\Phi^-\rangle$'s. Contrarily for $\omega = 0$, $|\Psi_\omega\rangle$ couples both the odd and even subspaces and homogeneously spreads over the entire Hilbert space at sufficiently long time.

To understand the nonequilibrium features of the initial state $|\Psi_\omega\rangle$, we monitor its survival probability [3,80,91–95], defined as

$$R(t) \equiv |\langle \Psi_\omega(t)|\Psi_\omega\rangle|^2 = \left|\sum_{j=\pm}\sum_{n=1}^{\frac{N}{2}} |c_n^j|^2 e^{-iE_n^j t}\right|^2. \tag{17}$$

Then, ensemble averaged survival probability can be expressed as [80]

$$\langle R(t)\rangle = \left\langle \int dE \mathcal{F}(E) e^{-iEt}\right\rangle + \overline{R},$$
$$\mathcal{F}(E) = \sum_{m\neq n,\{j,l\}=\pm} |c_m^j|^2 |c_n^l|^2 \delta\left(E - E_m^j + E_n^l\right), \tag{18}$$

where the equilibrium value of the survival probability $\overline{R}$ is the inverse participation ratio of the initial state $|\Psi_\omega\rangle$ in the energy eigenbasis and can be written as

$$\overline{R} = \left\langle \sum_{j=\pm}\sum_{n}^{\frac{N}{2}} |c_n^j|^4 \right\rangle$$
$$= \sum_{j=\pm}(1 + j\sin 2\omega)^2 \sum_{n=1}^{\frac{N}{2}} \left\langle \left|\Phi_n^j(k)\right|^4\right\rangle$$
$$\approx \frac{3(1+\sin^2 2\omega)}{N}, \tag{19}$$

where we used the fact that each of the diagonal blocks in a reduced SC matrix contributes ergodic eigenstates of length $\frac{N}{2}$ following the Haar distribution. Thus, energy eigenstate components of a random SC matrix follow the Porter-Thomas distribution [96,97] similar to the GOE. Equation (19) implies that $|\Psi_\omega\rangle$ can spread to the entire energy space or a part of it, depending on ω, where the maximal (minimal) spread occurs for $\omega = 0$ ($\omega = \pm\frac{\pi}{4}$).

The second term in Eq. (18) describes the nonequilibrium evolution of $|\Psi_\omega\rangle$ and can be evaluated following Ref. [80] since the eigenvalues are independent of the eigenstate components in the case of a random SC matrix. Then, the survival probability of the initial state in Eq. (14) has the following analytical expression:

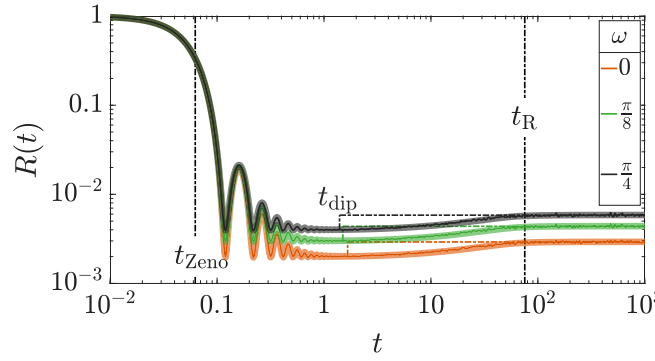


FIG. 2. Ensemble-averaged survival probability of $|\Psi_\omega\rangle$ [Eq. (14)] for random SC matrices with $N = 1024$ and various values of ω. For survival probability, solid lines denote numerical simulations and the bold curves follow the analytical expression in Eq. (20). Vertical black lines denote the Zeno and relaxation times, while correlation holes have been marked with dashed lines.

$$R_\omega(t) \approx (1-\overline{R})\left[\frac{\mathrm{J}_1(2\Gamma t)^2}{(\Gamma t)^2} - \frac{(1+\sin^2 2\omega)}{N} b_2^{\rm GOE}\left(\frac{t}{t_{\rm H}}\right)\right] + \overline{R}, \tag{20}$$

where $\mathrm{J}_1(x)$ is the Bessel function of the first kind of order 1, Γ is the width of the local density of states of $|\Psi_\omega\rangle$, $b_2^{\rm GOE}(\tau)$ is given in Eq. (10), $\overline{R}$ is given in Eq. (19), and $\tau \equiv \frac{t}{t_{\rm H}}$ is the dimensionless time, where $t_{\rm H}$ is the Heisenberg time,

$$t_{\rm H} \approx \frac{N}{\Gamma} = 2\sqrt{N}. \tag{21}$$

In Fig. 2, we verify the validity of Eq. (20) in the case of the initial states from Eq. (14). For $\omega = \pm\frac{\pi}{4}$, Eq. (20) describes the survival probability of a localized state in the case of a GOE matrix with dimension $\frac{N}{2}$.

The survival probability exhibits a universal quadratic decay $\sim 1 - \frac{N}{4}t^2$ for $t \ll t_{\rm Zeno}$ where the rate of decay is controlled by $\Gamma \approx \sqrt{N}/2$ and $t_{\rm Zeno} = 2/\sqrt{N}$ is the Zeno time [98]. At later times, $\langle R_\omega(t)\rangle$ exhibits oscillations with an envelope decaying as t^{-3}, a consequence of the energy bounds in the local density of states [87,99–102]. Such a power-law decay (called slope) leads to the dip of the survival probability, which can be found by expanding the first and second terms in $R_\omega(t)$ for long and short times, respectively, and finding the minimum of their sum,

$$\left.\frac{d}{dt}\left(\frac{1}{\pi(\Gamma t)^3} - \left(1 - \frac{2\Gamma t}{N}\right)\right)\right|_{t=t_{\rm dip}} = 0$$
$$\Rightarrow t_{\rm dip} = \left(\frac{24}{\pi(1+\sin^2 2\omega)}\right)^{\frac{1}{4}}. \tag{22}$$

Hence, dip time is independent of the system size but depends on the initial state. Beyond $t_{\rm dip}$, the survival probability exhibits a correlation hole dictated by the two-level form factor $b_2(\tau)$. At long time, $b_2(\tau)$ has a power-law decay [$b_2^{\rm GOE}(\tau) \sim 1/12\tau^2$], thus, we fix a small threshold,

ϵ such that

$$t_{\rm R} = \frac{1}{3}\sqrt{\frac{N}{\epsilon}}. \tag{23}$$

Hence, relaxation time is independent of ω and the same as that of the GOE [80]. Moreover, $t_{\rm R}$ has the same order of magnitude as that of the Heisenberg time, $t_{\rm H} \approx 2\sqrt{N}$. In Fig. 2, we show the different timescales for various values of γ. Eqs. (19) and (22) imply that the symmetric ($\omega = \pi/4$) and antisymmetric ($\omega = -\pi/4$) initial states are the quickest ones to reach the correlation hole with minimum spread over the energy space.

Long-lived initial states

As the energy spectrum of a random SC matrix is a superposition of two pure spectra from the GOE, the corresponding ground states $|\Phi_1^-\rangle$ and $|\Phi_1^+\rangle$ with uncorrelated energies E_1^- and E_1^+ (from odd and even sectors, respectively) are the global ground and first excited states of the entire spectrum with a high probability, and the lowest two energy levels of a SC matrix are most likely to be $E_1^\pm$. The gap between such energy levels follows the density

$$\mathrm{P}(s) = \frac{2}{\pi}\exp\left(-\frac{s^2}{\pi}\right), \tag{24}$$

valid for an integrable two-level system [28]. If we start from a superposition of the ground states from the two different symmetry sectors, then the system exhibits Rabi oscillations,

$$R(t) = |\langle\Psi_{\text{o-e}}(t)|\Psi_{\text{o-e}}\rangle|^2 = \cos^2\left(\frac{S_{\text{o-e}}}{2}t\right),$$
$$S_{\text{o-e}} \equiv |E_1^- - E_1^+|, \quad |\Psi_{\text{o-e}}\rangle \equiv \frac{|\Phi_1^-\rangle + |\Phi_1^+\rangle}{\sqrt{2}}, \tag{25}$$

with a time period $t_{\rm Rabi} = S_{\text{o-e}}^{-1}$. The density of the gap between E_1^- and E_1^+ [Eq. (24)] implies that they have a high probability to cluster, i.e., $|\Phi_1^-\rangle$ and $|\Phi_1^+\rangle$ can be almost degenerate such that $t_{\rm Rabi}$ is arbitrarily large. As a typical excitation takes $O(t_{\rm H})$ time to equilibrate, if

$$\frac{t_{\rm Rabi}}{t_{\rm H}} \sim O(N), \tag{26}$$

then the time period of the Rabi oscillation is so large that $|\Psi_{\text{o-e}}\rangle$ is effectively an equilibrium state, i.e., the system retains the memory of the initial configuration for a time period much larger than the Heisenberg time. This is illustrated in Fig. 3(a) for a single realization of a random SC matrix. Thus, similar to the symmetry-broken states in systems exhibiting quantum phase transition, i.e., transverse field Ising [103,104], Lipkin-Meshkov-Glick [35,36], collective models [39,40,105], $|\Psi_{\text{o-e}}\rangle$ breaks the exchange symmetry of a random SC matrix whenever the condition in Eq. (26) holds, which has a probability of occurring,

$$\int_0^{\frac{1}{N}} ds\mathrm{P}(s) = \mathrm{Erf}\left(\frac{1}{\sqrt{\pi}N}\right). \tag{27}$$

Hence, for a given SC matrix with finite system size, there is a finite probability $\approx\mathrm{Erf}(1/\sqrt{\pi}N)$ that $|\Psi_{\text{o-e}}\rangle$ behaves like a symmetry-broken state, i.e., an equilibrium state despite not being an energy eigenstate. In the thermodynamic limit ($N \to \infty$), $\mathrm{Erf}(1/\sqrt{\pi}N) = 2/\pi N + O(N^{-3})$ goes to zero such that the probability to find an SC matrix with a symmetry-broken state vanishes. Thus, spontaneous symmetry breaking occurs only for a vanishing fraction [$\approx O(N^{-1})$] of all possible random SC matrices.

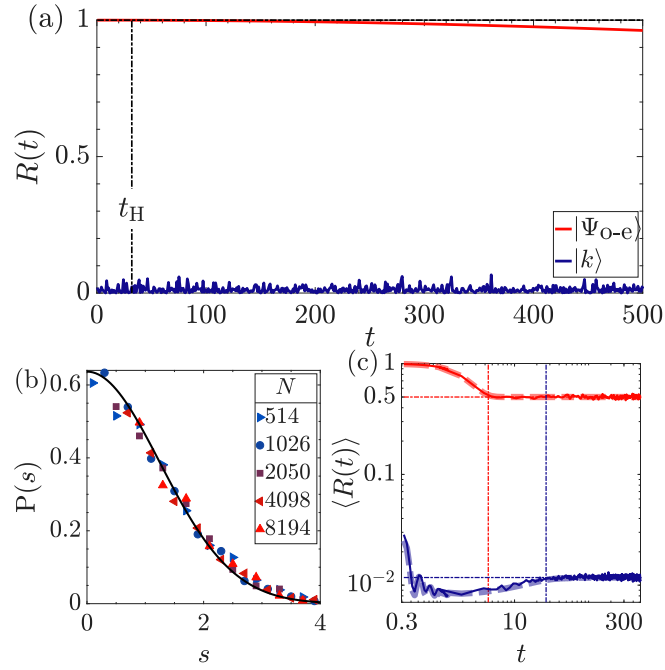


FIG. 3. (a) Survival probability of the superposition state $|\Psi_{\text{o-e}}\rangle$ [Eq. (25)] having energy $(E_1^- + E_1^+)/2$ and a unit vector $|k\rangle$ with similar energy for a single random SC matrix with $N = 256$. Vertical line denotes the Heisenberg time. Notice that $|\Psi_{\text{o-e}}\rangle$ is almost stationary even up to time $\approx O(10t_{\rm H})$ while $|k\rangle$ equilibrates at $t \approx t_{\rm H}$. (b) Density of $|E_1^- - E_1^+|$ upon unfolding for different system sizes, where the solid line corresponds to the 2×2 Poisson ensemble, Eq. (24). (c) Ensemble averaged survival probability of $|\Psi_{\text{o-e}}\rangle$ and $|k\rangle$ with respective analytical expressions from Eqs. (28) and (20) shown via dashed lines, where the vertical (horizontal) lines denote the relaxation times (equilibrium values).

The ensemble-averaged survival probability of $|\Psi_{\text{o-e}}\rangle$ can be expressed as

$$\begin{aligned}\langle R(t)\rangle &= \int_0^\infty dS_{\text{o-e}}\mathrm{P}(S_{\text{o-e}})R(t)\\ &= \int_0^\infty ds\frac{2}{\pi}e^{-\frac{s^2}{\pi}}\cos^2\left(\frac{\langle S_{\text{o-e}}\rangle s}{2}t\right)\\ &= \frac{1}{2} + \frac{1}{2}\exp\left(-\frac{\pi\langle S_{\text{o-e}}\rangle^2}{4}t^2\right),\end{aligned} \tag{28}$$

which exhibits a Gaussian decay with a rate $\sqrt{\pi}\langle S_{\text{o-e}}\rangle/2$ before saturating to $\overline{R} = 1/2$. Such a Gaussian decay relaxes at the time $t_{\rm R} = \frac{2}{\langle S_{\text{o-e}}\rangle}\sqrt{|\ln\epsilon|/\pi}$ given a tolerance value $\epsilon \ll 1$. Since $\langle S_{\text{o-e}}\rangle$ is smaller than the global bandwidth Γ, comparing with Eq. (20), we find that the average survival probability of $|\Psi_{\text{o-e}}\rangle$ has a much slower decay but a smaller relaxation time compared with a localized state with similar energy, as shown in Fig. 3(c).

IV. EQUILIBRATION IN SC ENSEMBLE

So far, we looked at the unitary time evolution of an initial state and obtained the corresponding survival probability and associated timescales for a random SC matrix. In our analyses, averaging the dynamics over an ensemble ensured equilibration at sufficiently long time due to decoherence [106]. However, the Poincaré recurrence theorem dictates that, for a single Hamiltonian of finite dimension, the time-reversal invariance of a unitary dynamics for a discrete spectrum leads to recurrences with a time period proportional to the Heisenberg timescale [107–109]. Such quantum revivals [110] have been demonstrated in case of the hydrogen atom [111]. Nevertheless, closed quantum systems can attain equilibrium in the sense that given a local operator O, its expectation value can remain arbitrarily close to the infinite time average for a finite interval of time beyond the relaxation time until a recurrence occurs [112]. Particularly, the quantity $|\langle \mathsf{O}(t)\rangle - \mathrm{Tr}\bar{\rho}\mathsf{O}|$ can remain arbitrarily small in said time window, where

$$\bar{\rho} \equiv \lim_{T\to\infty} \frac{1}{T}\int_0^T dt\, |\Psi(t)\rangle\langle\Psi(t)| \tag{29}$$

is the equilibrium density matrix possessing maximum possible entropy subject to all the conserved charges of the system [71,113]. Such equilibration is rigorously proven for many-body systems provided the local correlations with respect to the initial state decay sufficiently fast [114,115].

To study the relaxation of an observable with respect to an SC matrix, we initialize our system in the state $|\Psi_\omega\rangle$ [Eq. (14)] and look at the time evolution of the expectation value of an observable O:

$$\begin{aligned}\mathsf{O}(t) &\equiv \langle\Psi_\omega(t)|\mathsf{O}|\Psi_\omega(t)\rangle \\ &= \sum_{j,l=\pm}\sum_{m\neq n} \left(c_m^j\right)^\star c_n^l \langle\Phi_m^j|\mathsf{O}|\Phi_n^l\rangle e^{-i(E_m^j - E_n^l)t} \\ &\quad + \sum_{j=\pm}\sum_n |c_n^j|^2 \langle\Phi_n^j|\mathsf{O}|\Phi_n^j\rangle,\end{aligned} \tag{30}$$

where $c_n^\pm \equiv \langle\Phi_n^\pm|\Psi_\omega\rangle$. Equation (29) implies that the expectation value of the observable equilibrates to the infinite time average,

$$\langle\mathsf{O}\rangle_{\mathrm{DE}} \equiv \sum_{j=\pm}\sum_n |c_n^j|^2 \mathsf{O}_{nn}^j, \quad \mathsf{O}_{nn}^\pm \equiv \langle\Phi_n^\pm|\mathsf{O}|\Phi_n^\pm\rangle, \tag{31}$$

which is also known as the average with respect to the diagonal ensemble [9,70,116]. As equilibration is constrained by the conserved quantities, we need to consider all the constants of motion to describe the equilibration process. In a system governed by a time-independent Hamiltonian, the energy is always conserved. For example, $|\Psi_\omega\rangle$, the initial state in Eq. (14), has an energy

$$\langle E\rangle \equiv \langle\Psi_\omega|H|\Psi_\omega\rangle = \sum_{j=\pm}\sum_n (1 + j\sin 2\omega)\left|\Phi_n^j(k)\right|^2 E_n^j, \tag{32}$$

which is conserved at all times, during the nonequilibrium evolution as well as beyond t_{R} when $|\Psi_\omega(t)\rangle$ equilibrates to the maximum entropy state.

In the absence of any conserved quantity other than energy, i.e., in a completely chaotic system, we expect ergodicity to hold, i.e., at least the bulk energy states are uniformly distributed on a hypersphere. In a classical system, ergodicity implies the equivalence of the infinite time average and the microcanonical average over the constant energy surface in the phase space [117–119]. Similarly, in an ergodic quantum system, typicality arguments [120–124] imply that the infinite time average of O coincides with the average with respect to the microcanonical ensemble, which in the case of the SC matrix is

$$\langle\mathsf{O}\rangle_{\mathrm{ME}} = \frac{1}{N_\Delta}\sum_{E_n^+, E_n^- \in \Delta} \mathsf{O}_{nn}^- + \mathsf{O}_{nn}^+, \tag{33}$$

where $\Delta \equiv [\langle E\rangle - \Delta_E, \langle E\rangle + \Delta_E]$ is a microcanonical energy shell around the energy of the initial state containing $1 \ll N_\Delta \ll N$ energy levels over which the density of states varies sufficiently slowly. Importantly, the microcanonical average at a given energy is independent of the choice of the initial state. The equivalence of microcanonical and diagonal averages is shown in quantum systems with few degrees of freedom [125,126].

As the local operator O acts on a small part $\mathcal{H}_A$ of the entire Hilbert space, the complementary subspace acts as a heat bath for $\mathcal{H}_A$ [127]. Then, the microcanonical average is equal to the canonical expectation value [10,128]:

$$\langle\mathsf{O}\rangle_{\mathrm{GE}} \equiv \mathrm{Tr}\{\hat{\rho}_{\mathrm{GE}}\hat{\mathsf{O}}\}, \quad \hat{\rho}_{\mathrm{GE}} \equiv \frac{e^{-\frac{\hat{H}}{T}}}{\mathrm{Tr}[e^{-\frac{\hat{H}}{T}}]}, \tag{34}$$

where $\hat{\rho}_{\mathrm{GE}}$ is the equilibrium thermal density matrix with a canonical partition function $\mathrm{Tr}[e^{-\frac{\hat{H}}{T}}]$ and T is the effective temperature of the initial state following conservation of energy in Eq. (32)

$$\langle E\rangle = \mathrm{Tr}\{\hat{\rho}_{\mathrm{GE}}\hat{H}\} = \frac{\mathrm{Tr}\{\hat{H}e^{-\frac{\hat{H}}{T}}\}}{\mathrm{Tr}\{e^{-\frac{\hat{H}}{T}}\}}. \tag{35}$$

Thus, the Gibbs ensemble allows one to assign a temperature to an initial state [76], which determines the size of the microcanonical energy window around $\langle E\rangle$ [6]. Note that, in many-body systems with U(1) symmetry, the Gibbs ensemble is defined with an additional Lagrange multiplier for the particle number conservation [9]. In our case, the SC matrix can be understood as a matrix model of a single-particle closed system where particle number is trivially conserved and becomes the identity matrix in the site basis.

In case of highly excited initial states and observables not respecting the exchange symmetry, energy conservation alone [Eq. (34)] is sufficient to get the thermal expectation value describing the equilibrium behavior. However, in general, the presence of a global symmetry implies that the Gibbs ensemble needs an additional Lagrange multiplier other than the inverse temperature to describe the maximum entropy density matrix [9,45,70–72,114,116,129]

$$\begin{aligned}\langle\mathsf{O}\rangle_{\mathrm{GE}} &\equiv \mathrm{Tr}\hat{\rho}_{\mathrm{GE}}\hat{\mathsf{O}}, \quad \hat{\rho}_{\mathrm{GE}} \equiv \frac{e^{-\frac{H-\mu\mathsf{J}}{T}}}{Z}, \\ Z &= \mathrm{Tr}e^{-\frac{H-\mu\mathsf{J}}{T}} = \sum_{j=\pm}\sum_{n=1}^{\frac{N}{2}} e^{-\frac{E_n^j - j\mu}{T}},\end{aligned} \tag{36}$$

where Z is the partition function. The Lagrange multipliers μ and T^{-1} are constrained by the conservation of energy and exchange symmetry, hence, satisfy the following two equations:

$$\langle E\rangle = \mathrm{Tr}\hat{\rho}_{\mathrm{GE}}\hat{H} = \frac{\sum_{j=\pm}\sum_{n=1}^{\frac{N}{2}} E_n^j e^{-\frac{E_n^j - j\mu}{T}}}{Z},$$
$$\langle \mathsf{J}\rangle = \mathrm{Tr}\hat{\rho}_{\mathrm{GE}}\hat{\mathsf{J}} = \frac{\sum_{j=\pm} j\sum_{n=1}^{\frac{N}{2}} e^{-\frac{E_n^j - j\mu}{T}}}{Z}, \tag{37}$$

where $\langle E\rangle$ is energy [Eq. (32)] and $\langle \mathsf{J}\rangle = \sin 2\omega$ [Eq. (15)] is the expectation value of the exchange operator with respect to the initial state $|\Psi_\omega\rangle$. Expanding in the energy eigenbasis, we can express the thermal average $\langle \mathsf{O}\rangle_{\mathrm{GE}}$ as

$$\langle \mathsf{O}\rangle_{\mathrm{GE}} = \frac{\sum_{j=\pm}\sum_{n=1}^{\frac{N}{2}} \mathsf{O}_{nn}^j e^{-\frac{E_n^j - j\mu}{T}}}{Z}. \tag{38}$$

In integrable and nonergodic systems, extensively many conserved charges generalize the Gibbs ensemble to have multiple Lagrange multipliers, as demonstrated in many-body systems [130–139] and field theories [129,140–142].

The equivalence of the infinite time average from Eq. (31) to the canonical average in Eq. (38) implies thermalization, i.e., the equilibrium state remains arbitrarily close to the thermal state, $\hat{\rho}_{\mathrm{GE}}$ beyond relaxation time. This motivated the eigenstate thermalization hypothesis (ETH) [2–6,10,128,143], which dictates that in an ergodic closed quantum system with eigenpairs $\{E_n, \Phi_n\}$, the matrix elements of an observable follow the ansatz

$$\langle\Phi_m|\hat{\mathsf{O}}|\Phi_n\rangle = \mathsf{O}(\overline{E})\delta_{mn} + \frac{1}{\sqrt{\rho(\overline{E})}}\mathcal{F}(\overline{E},\omega)\mathcal{R}_{mn}, \tag{39}$$

where $\overline{E} = (E_m + E_n)/2$, $\omega = E_n - E_m$, $\mathsf{O}(\overline{E})$ and $\mathcal{F}(\overline{E},\omega)$ are smooth functions of their arguments, $\rho(E)$ is the density of states, and $\mathcal{R}_{mn}$ is a random number with zero mean and unit variance. The ETH ansatz also implies that the microcanonical [Eq. (33)], canonical [Eq. (36)], and equilibrium [Eq. (31)] expectation values of a generic local observable coincide. Note that, despite being integrable, certain translationally invariant finite-range quantum systems may satisfy ETH in the weak sense [124].

To probe the validity of ETH in case of a random SC matrix, we obtain the expectation values of various local observables after initializing our system in a state $|\Psi_\omega\rangle$ [Eq. (14)]. The density of states of an SC matrix is symmetric about the zero energy, hence, the energy of the initial state [Eq. (32)] is $\approx O(1)$, lies in the middle of the spectrum while the spectral bandwidth scales as $O(\sqrt{N})$. Thus, our chosen initial states are highly excited. The semicircle law implies that, within the energy window $\langle E\rangle \pm \Delta_E$ around zero energy, there exists $O(\Delta_E\sqrt{N})$ number of energy levels. Thus, such an energy window can be considered to be a microcanonical shell. In our numerical results, we choose $\Delta_E = 0.02$.

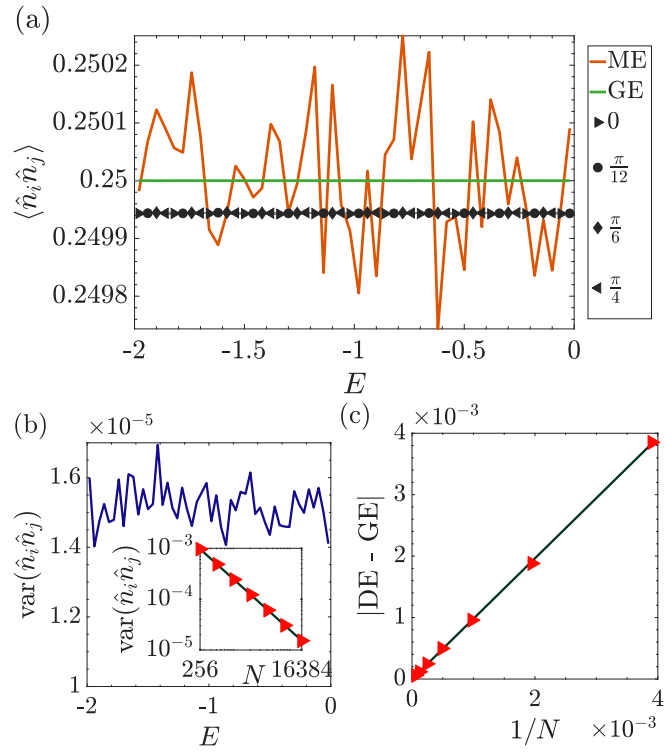


FIG. 4. (a) Expectation of density-density correlation [Eq. (40)] with respect to microcanonical ensemble (ME) and Gibbs ensemble (GE) for $N = 16384$, $i = 1$, $j = \frac{L}{2}$ ($N = 2^L$) averaged over 256 disorder realizations. The microcanonical average is done over windows of width 0.04 in the energy units. Markers denote the average with respect to the diagonal ensemble (DE) for different initial states parametrized by ω [Eq. (14)]. (b) Variance of the diagonal terms of the density-density correlation in the energy basis within microcanonical windows. Inset shows the variance with respect to system size, where the solid line is a linear fit on a log-log scale with slope ≈ -1. (c) Difference of the averages with respect to diagonal and Gibbs ensembles as a function of inverse system size. Solid line denotes a linear fit with intercept ≈ 0.

First, we look at the correlation between the number densities at the ith and jth sites of a fictitious 1D lattice,

$$\hat{\mathsf{O}} = \hat{n}_i\hat{n}_j, \quad \hat{n} = \frac{\hat{\mathbb{I}} - \hat{\sigma^z}}{2}, \tag{40}$$

assuming that the matrix H is the Fock-space representation of a spin-$\frac{1}{2}$ chain with L number of sites, $N = 2^L$. Such a local operator does not commute with the exchange matrix J. As the eigenstates are Haar random vectors other than the $\mathbb{Z}_2$ symmetry, we expect that the site occupations are homogeneous over the lattice, $\langle\hat{n}_i\rangle \approx \frac{1}{2}$ for all lattice indices and independent of each other. Then, $\langle\hat{n}_i\hat{n}_j\rangle = \langle\hat{n}_i\rangle\langle\hat{n}_j\rangle \approx \frac{1}{4}$, irrespective of the choice of initial states.

In Fig. 4(a), we show the expectation value of the density-density correlation with respect to different ensembles as a function of the energy of $|\Psi_\omega\rangle$. As the observable does not respect the global symmetry of the Hamiltonian, the equilibrium value (average with respect to the diagonal ensemble) does not depend on the choice of the initial state, as shown for different values of ω in Fig. 4(a). The microcanonical

average fluctuates around the expected value of $\langle \hat{n}_i \hat{n}_j \rangle = \frac{1}{4}$. In Fig. 4(b), we show that the variance of the diagonal terms of the density-density correlation within microcanonical shells decays linearly with the system size. Thus, the diagonal ETH ansatz [Eq. (39)] is valid for our observable.

As the energy of the initial state is close to the middle of the spectrum, we expect equipartition of energy states with Gibbs weight $\approx N^{-1}$ such that the thermal average must coincide with the microcanonical average, as shown in Fig. 4(a). We find a small difference between the averages with respect to diagonal and canonical ensembles for finite system sizes. Such a difference decays linearly with N^{-1} and vanishes in the limit $N \to \infty$, as shown in Fig. 4(c). Note that, as $\hat{n}_i \hat{n}_j$ do not commute with J, energy conservation alone is sufficient to get the thermal expectation values as in Eq. (34). Thus, we find that the expectation values with respect to microcanonical, canonical, and diagonal ensembles coincide for the density-density correlation, validating thermalization.

Next, we look at the kinetic-energy operator of 1D single-particle systems [22]

$$\hat{\mathrm{KE}} = -\sum_{k=1}^{N-1} \hat{c}_k^\dagger \hat{c}_{k+1} + \hat{c}_{k+1}^\dagger \hat{c}_k, \tag{41}$$

where $\hat{c}_j^\dagger$ ($\hat{c}_j$) is the creation (annihilation) operator on the jth site of a 1D tight-binding model. In the site basis, $\{|k\rangle\}$, the above operator is tridiagonal with zero diagonal. Importantly, $\hat{\mathrm{KE}}|k\rangle = |N-k+1\rangle$ such that $[\hat{\mathrm{KE}}, \mathrm{J}] = 0$.

In Figs. 5(a) and 5(b), we show the expectation value of the kinetic energy with respect to various ensembles for two different values of ω. The average with respect to the Gibbs ensemble is computed following the conservation of both energy and exchange symmetry as in Eq. (36). As the observable respects the global symmetry of the Hamiltonian, the equilibrium value depends on the choice of the initial state, unlike the density-density correlation. While for finite system sizes, we see a difference between the canonical average and equilibrium value, such a difference decays linearly with system size as shown in Figs. 5(c) and 5(d). Moreover, the fluctuations of the diagonal terms within microcanonical windows also vanish in the thermodynamic limit on par with the ETH ansatz, as shown in the insets of Figs. 5(c) and 5(d).

Thus, the kinetic-energy operator also exhibits thermalization in the case of random SC matrices despite respecting the global symmetry of the Hamiltonian. Similar behavior is observed in the case of the following operator:

$$\mathrm{J}_{\mathrm{loc}} = \mathbb{I}^{\frac{N-4}{2}\times\frac{N-4}{2}} \oplus \mathrm{J}^{4\times4} \oplus \mathbb{I}^{\frac{N-4}{2}\times\frac{N-4}{2}}, \tag{42}$$

which commutes with the global exchange symmetry and exhibits thermalization, as shown in Fig. 6.

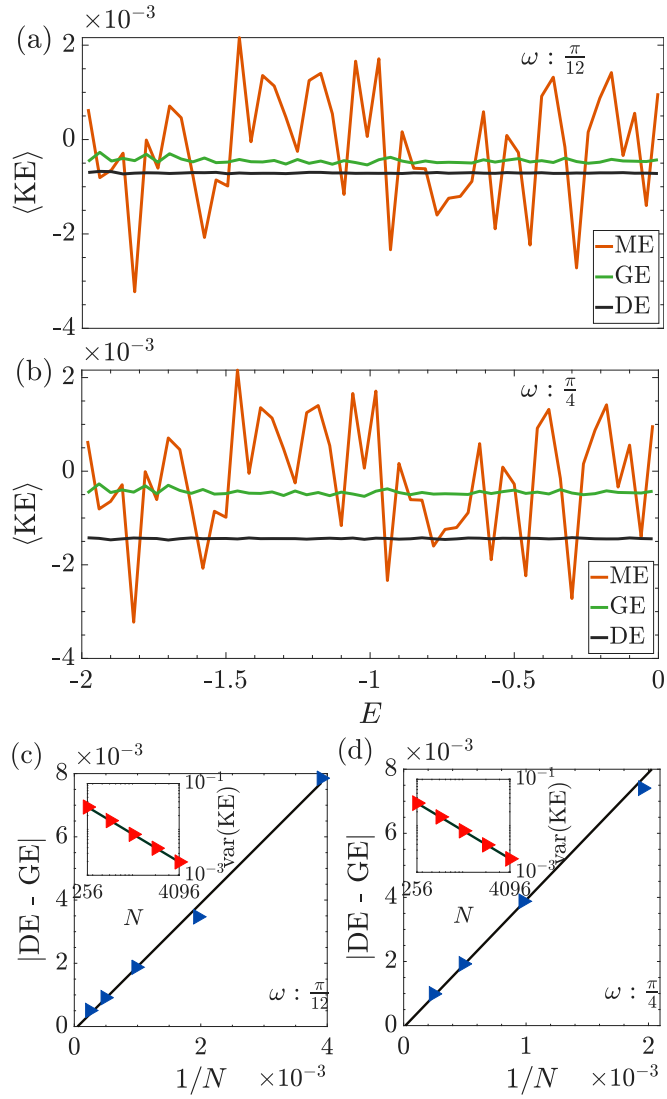


FIG. 5. Expectation of kinetic energy operator [Eq. (41)] with respect to microcanonical ensemble (ME), Gibbs ensemble (GE), and digonal ensemble (DE) for (a) $\omega = \frac{\pi}{12}$ and (b) $\omega = \frac{\pi}{4}$ with $N = 4096$ averaged over 1024 disorder realizations. ω characterizes the initial state [Eq. (14)]. Difference of the averages with respect to diagonal and Gibbs ensembles as a function of inverse system size for (c) $\omega = \frac{\pi}{12}$ and (d) $\omega = \frac{\pi}{4}$. Solid line denotes a linear fit with intercept ≈ 0. Insets show the variance of the diagonal terms of the kinetic energy operator in the energy basis within microcanonical windows, where the solid line is a linear fit in log-log scale with slope ≈ -1.

V. DISCUSSION

In this work, we look at the random SC matrix, which has a discrete $\mathbb{Z}_2$ symmetry and commutes with the exchange symmetry operator. The corresponding Hilbert space can be split into two decoupled subspaces, namely, odd (spanned by antisymmetric states) and even (spanned by symmetric states) sectors. The energy spectrum of an SC matrix is a superposition of two pure spectra; hence, we can analytically describe the energy correlations, i.e., the level spacing distribution and number variance.

To understand the dynamical properties of random SC matrices, we consider the initial state $|\Psi_\omega\rangle$, which is a function of $-\frac{\pi}{2} \leqslant \omega \leqslant \frac{\pi}{2}$ and a weighted superposition of the exchange doublets. Depending on the value of ω, the initial state can be confined in the odd or even sector or can couple these subspaces as well. We analytically obtain the survival probability (i.e., the probability of the system returning to its initial configuration) of $|\Psi_\omega\rangle$, corresponding equilibrium value, and characteristic timescales. The survival probability exhibits a

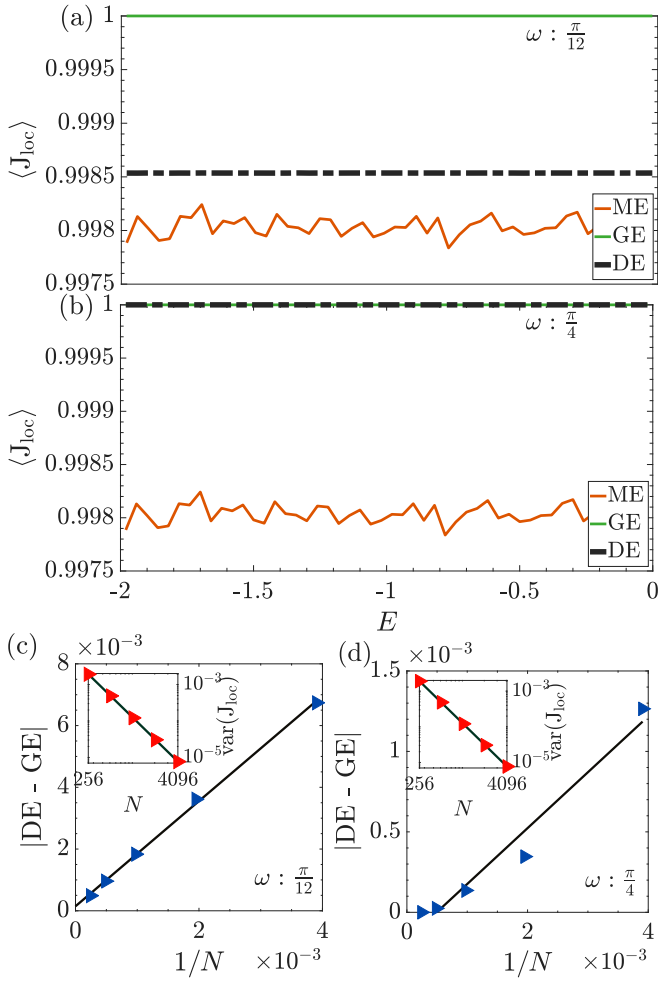


FIG. 6. Expectation of the operator in Eq. (42) with respect to the microcanonical ensemble (ME), Gibbs ensemble (GE), and diagonal ensemble (DE) for (a) $\omega = \frac{\pi}{12}$ and (b) $\omega = \frac{\pi}{4}$ with $N = 4096$ averaged over 1024 disorder realizations. ω characterizes the initial state [Eq. (14)]. Difference of the averages with respect to diagonal and Gibbs ensembles as a function of inverse system size for (c) $\omega = \frac{\pi}{12}$ and (d) $\omega = \frac{\pi}{4}$. Solid line denotes linear fit with intercept ≈0. Insets show the variance of the diagonal terms of the kinetic-energy operator in the energy basis within microcanonical windows, where the solid line is a linear fit in log-log scale with slope ≈ -1.

correlation hole for all values of ω, indicating the presence of long-range correlation in the energy spectrum. However, the symmetric ($\omega = \frac{\pi}{4}$) and antisymmetric ($\omega = -\frac{\pi}{4}$) states take the smallest amount of time to reach the correlation hole and have the minimal spread over the energy space. Next, we look at the initial state $|\Psi_{\text{o-e}}\rangle$, which is a superposition of the local ground states of the two decoupled subspaces. We show that $|\Psi_{\text{o-e}}\rangle$ is a symmetry-broken state for a measure-zero fraction of random SC matrices with spontaneous symmetry breaking in the thermodynamic limit.

To understand the thermalization in the case of SC matrices, we consider initial states and local observables that do and do not respect the global symmetry of the Hamiltonian. By comparing the equilibrium expectation value, microcanonical and canonical averages of the local observables, we show that thermalization takes place in the case of random SC matrices. We show that the equilibrium behavior is dependent on the choice of initial state if the observable respects the global symmetry of the Hamiltonian and well described by the Gibbs ensemble for all the choices of initial state and observables.

As a future direction, we would like to explore deep thermalization [144,145] in the case of SC matrices, which is a stronger notion of thermalization where the projections of a time-evolved initial state spread uniformly over a subspace. It has been shown that, in the presence of a global symmetry (e.g., Sachdev-Ye-Kitaev model), higher moments of the projected ensemble can deviate from the Haar ensemble, indicating the absence of deep thermalization despite ETH remaining valid [17]. The SC matrix can serve as a minimal toy model to exhibit this phenomenon. One can also look at the dynamics of $|\Psi_\omega\rangle$ and thermalization in the case of the deformed centrosymmetric ensemble [31], where the extent of centrosymmetry can be tuned. The dependence of the relaxation times of various initial states on the strength of a symmetry-breaking perturbation can provide important insights into the equilibration of disordered systems.

ACKNOWLEDGMENTS

We sincerely thank Anandamohan Ghosh and Achilleas Lazarides for useful discussions and constructive criticism of the paper. A.K.D. acknowledges the support from the Leverhulme Trust Research Project Grant No. RPG-2025-063. All the computations were performed in the Kepler Computing facility of the Department of Physical Sciences, IISER Kolkata, India.

DATA AVAILABILITY

The data that support the findings of this article are openly available [146].

[1] For a Hilbert space with dimension N, an ergodic state is uniformly distributed in the $(N-1)$-dimension unit hypersphere [147,148].

[2] M. Srednicki, Chaos and quantum thermalization, Phys. Rev. E **50**, 888 (1994).

[3] A. Polkovnikov, K. Sengupta, A. Silva, and M. Vengalattore, *Colloquium*: Nonequilibrium dynamics of closed interacting quantum systems, Rev. Mod. Phys. **83**, 863 (2011).

[4] R. Nandkishore and D. A. Huse, Many-body localization and thermalization in quantum statistical mechanics, Annu. Rev. Condens. Matter Phys. **6**, 15 (2015).

[5] F. Borgonovi, F. Izrailev, L. Santos, and V. Zelevinsky, Quantum chaos and thermalization in isolated systems of interacting particles, Phys. Rep. **626**, 1 (2016).

[6] J. M. Deutsch, Eigenstate thermalization hypothesis, Rep. Prog. Phys. **81**, 082001 (2018).

[7] E. J. Torres-Herrera and L. F. Santos, Extended nonergodic states in disordered many-body quantum systems, Ann. Phys. (Berlin, Ger.) **529**, 1600284 (2017).

[8] M. Pino, L. B. Ioffe, and B. L. Altshuler, Nonergodic metallic and insulating phases of Josephson junction chains, Proc. Natl. Acad. Sci. USA **113**, 536 (2016).

[9] L. Vidmar and M. Rigol, Generalized Gibbs ensemble in integrable lattice models, J. Stat. Mech. (2016) 064007.

[10] T. Mori, T. N. Ikeda, E. Kaminishi, and M. Ueda, Thermalization and prethermalization in isolated quantum systems: A theoretical overview, J. Phys. B: At. Mol. Opt. Phys. **51**, 112001 (2018).

[11] C. J. Turner, A. A. Michailidis, D. A. Abanin, M. Serbyn, and Z. Papić, Weak ergodicity breaking from quantum many-body scars, Nat. Phys. **14**, 745 (2018).

[12] S. Sinha and S. Sinha, Chaos and quantum scars in Bose-Josephson junction coupled to a bosonic mode, Phys. Rev. Lett. **125**, 134101 (2020).

[13] H. Dong, J.-Y. Desaules, Y. Gao, N. Wang, Z. Guo, J. Chen, Y. Zou, F. Jin, X. Zhu, P. Zhang, H. Li, Z. Wang, Q. Guo, J. Zhang, L. Ying, and Z. Papić, Disorder-tunable entanglement at infinite temperature, Sci. Adv. **9**, eadj3822 (2023).

[14] A. Pizzi, L.-H. Kwan, B. Evrard, C. B. Dag, and J. Knolle, Genuine quantum scars in many-body spin systems, Nat. Commun. **16**, 6722 (2025).

[15] S. Roy and A. Lazarides, Strong ergodicity breaking due to local constraints in a quantum system, Phys. Rev. Res. **2**, 023159 (2020).

[16] K. Royen, S. Mondal, F. Pollmann, and F. Heidrich-Meisner, Enhanced many-body localization in a kinetically constrained model, Phys. Rev. E **109**, 024136 (2024).

[17] T. Bhore, J.-Y. Desaules, and Z. Papić, Deep thermalization in constrained quantum systems, Phys. Rev. B **108**, 104317 (2023).

[18] A. K. Das and A. Lazarides, Ground state and persistent oscillations in the quantum east model, arXiv:2602.23422.

[19] M. Serbyn, Z. Papić, and D. A. Abanin, Local conservation laws and the structure of the many-body localized states, Phys. Rev. Lett. **111**, 127201 (2013).

[20] O. Shtanko, D. S. Wang, H. Zhang, N. Harle, A. Seif, R. Movassagh, and Z. Minev, Uncovering local integrability in quantum many-body dynamics, Nat. Commun. **16**, 2552 (2025).

[21] A. K. Kulshreshtha, A. Pal, T. B. Wahl, and S. H. Simon, Behavior of l-bits near the many-body localization transition, Phys. Rev. B **98**, 184201 (2018).

[22] P. Łydżba, Y. Zhang, M. Rigol, and L. Vidmar, Single-particle eigenstate thermalization in quantum-chaotic quadratic Hamiltonians, Phys. Rev. B **104**, 214203 (2021).

[23] R. Modak, S. Mukerjee, E. A. Yuzbashyan, and B. S. Shastry, Integrals of motion for one-dimensional Anderson localized systems, New J. Phys. **18**, 033010 (2016).

[24] A. K. Das, A. Ghosh, and I. M. Khaymovich, Absence of mobility edge in short-range uncorrelated disordered model: Coexistence of localized and extended states, Phys. Rev. Lett. **131**, 166401 (2023).

[25] A. K. Das and A. Ghosh, Nonergodic extended states in the β ensemble, Phys. Rev. E **105**, 054121 (2022).

[26] A. K. Das, A. Ghosh, and I. M. Khaymovich, Robust nonergodicity of the ground states in the β ensemble, Phys. Rev. B **109**, 064206 (2024).

[27] A. K. Das, A. Ghosh, and I. M. Khaymovich, Emergent multifractality in power-law decaying eigenstates, Phys. Rev. B **112**, 024201 (2025).

[28] A. K. Das and A. Ghosh, Eigenvalue statistics for generalized symmetric and Hermitian matrices, J. Phys. A: Math. Theor. **52**, 395001 (2019).

[29] A. K. Das and A. Ghosh, Dynamical signatures of chaos to integrability crossover in 2×2 generalized random matrix ensembles, J. Phys. A: Math. Theor. **56**, 495003 (2023).

[30] M. V. Berry and P. Shukla, Spacing distributions for real symmetric 2×2 generalized Gaussian ensembles, J. Phys. A: Math. Theor. **42**, 485102 (2009).

[31] A. K. Das and A. Ghosh, Transport in deformed centrosymmetric networks, Phys. Rev. E **106**, 064112 (2022).

[32] A. K. Das and A. Ghosh, Chaos due to symmetry-breaking in deformed Poisson ensemble, J. Stat. Mech. (2022) 063101.

[33] A. Dutta, G. Aeppli, B. K. Chakrabarti, U. Divakaran, T. F. Rosenbaum, and D. Sen, *Quantum Phase Transitions in Transverse Field Spin Models: From Statistical Physics to Quantum Information* (Cambridge University Press, Cambridge, 2015).

[34] D. Mondal, S. Sinha, and S. Sinha, Chaos and quantum scars in a coupled top model, Phys. Rev. E **102**, 020101(R) (2020).

[35] Q. Wang and F. Pérez-Bernal, Signatures of excited-state quantum phase transitions in quantum many-body systems: Phase space analysis, Phys. Rev. E **104**, 034119 (2021).

[36] O. Castaños, R. López-Peña, J. G. Hirsch, and E. López-Moreno, Classical and quantum phase transitions in the Lipkin-Meshkov-Glick model, Phys. Rev. B **74**, 104118 (2006).

[37] L. F. Santos, M. Távora, and F. Pérez-Bernal, Excited-state quantum phase transitions in many-body systems with infinite-range interaction: Localization, dynamics, and bifurcation, Phys. Rev. A **94**, 012113 (2016).

[38] P. Pérez-Fernández, A. Relaño, J. M. Arias, P. Cejnar, J. Dukelsky, and J. E. García-Ramos, Excited-state phase transition and onset of chaos in quantum optical models, Phys. Rev. E **83**, 046208 (2011).

[39] M. Kloc, P. Stránský, and P. Cejnar, Quantum quench dynamics in Dicke superradiance models, Phys. Rev. A **98**, 013836 (2018).

[40] M.-J. Hwang, R. Puebla, and M. B. Plenio, Quantum phase transition and universal dynamics in the Rabi model, Phys. Rev. Lett. **115**, 180404 (2015).

[41] T. Kinoshita, T. Wenger, and D. S. Weiss, A quantum Newton's cradle, Nature (London) **440**, 900 (2006).

[42] S. Hofferberth, I. Lesanovsky, B. Fischer, T. Schumm, and J. Schmiedmayer, Non-equilibrium coherence dynamics in one-dimensional Bose gases, Nature (London) **449**, 324 (2007).

[43] M. Gring, M. Kuhnert, T. Langen, T. Kitagawa, B. Rauer, M. Schreitl, I. Mazets, D. A. Smith, E. Demler, and J. Schmiedmayer, Relaxation and prethermalization in an isolated quantum system, Science **337**, 1318 (2012).

[44] T. Langen, S. Erne, R. Geiger, B. Rauer, T. Schweigler, M. Kuhnert, W. Rohringer, I. E. Mazets, T. Gasenzer, and J. Schmiedmayer, Experimental observation of a generalized Gibbs ensemble, Science **348**, 207 (2015).

[45] K. Mallayya and M. Rigol, Prethermalization, thermalization, and Fermi's golden rule in quantum many-body systems, Phys. Rev. B **104**, 184302 (2021).

[46] P. Krupchitsky and V. Kisin, *Fundamental Research with Polarized Slow Neutrons* (Springer, Berlin Heidelberg, 2014).

[47] G. E. Mitchell, E. G. Bilpuch, P. M. Endt, and J. F. Shriner, Broken symmetries and chaotic behavior in ^{26}A, Phys. Rev. Lett. **61**, 1473 (1988).

[48] T. Guhr and H. Weidenmüller, Isospin mixing and spectral fluctuation properties, Ann. Phys. (NY) **199**, 412 (1990).

[49] A. Adams, G. Mitchell, and J. Shriner Jr., Statistical distribution of reduced transition probabilities in ^{26}Al, Phys. Lett. B **422**, 13 (1998).

[50] T. Scholak, F. de Melo, T. Wellens, F. Mintert, and A. Buchleitner, Efficient and coherent excitation transfer across disordered molecular networks, Phys. Rev. E **83**, 021912 (2011).

[51] T. Zech, R. Mulet, T. Wellens, and A. Buchleitner, Centrosymmetry enhances quantum transport in disordered molecular networks, New J. Phys. **16**, 055002 (2014).

[52] A. Ortega, T. Stegmann, and L. Benet, Efficient quantum transport in disordered interacting many-body networks, Phys. Rev. E **94**, 042102 (2016).

[53] C. Ellegaard, T. Guhr, K. Lindemann, J. Nygård, and M. Oxborrow, Symmetry breaking and spectral statistics of acoustic resonances in quartz blocks, Phys. Rev. Lett. **77**, 4918 (1996).

[54] K. Schaadt, A. P. B. Tufaile, and C. Ellegaard, Chaotic sound waves in a regular billiard, Phys. Rev. E **67**, 026213 (2003).

[55] J. X. de Carvalho, M. S. Hussein, M. P. Pato, and A. J. Sargeant, Symmetry-breaking study with deformed ensembles, Phys. Rev. E **76**, 066212 (2007).

[56] J. X. de Carvalho, S. Jalan, and M. S. Hussein, Deformed Gaussian-orthogonal-ensemble description of small-world networks, Phys. Rev. E **79**, 056222 (2009).

[57] S. Jalan, Spectral analysis of deformed random networks, Phys. Rev. E **80**, 046101 (2009).

[58] P. Facchi and S. Pascazio, Quantum Zeno subspaces, Phys. Rev. Lett. **89**, 080401 (2002).

[59] L. F. Santos, F. Borgonovi, and G. L. Celardo, Cooperative shielding in many-body systems with long-range interaction, Phys. Rev. Lett. **116**, 250402 (2016).

[60] A. Gersho, Adaptive equalization of highly dispersive channels for data transmission, Bell Syst. Tech. J. **48**, 55 (1969).

[61] F. Magee and J. Proakis, An estimate of the upper bound on error probability for maximum-likelihood sequence estimation on channels having a finite-duration pulse response (Corresp.), IEEE Trans. Inf. Theory **19**, 699 (1973).

[62] L. Datta and S. D. Morgera, On the reducibility of centrosymmetric matrices—applications in engineering problems, Circuits Syst. Signal Proces. **8**, 71 (1989).

[63] P. Gaudreau and H. Safouhi, Centrosymmetric matrices in the sinc collocation method for Sturm-Liouville problems, EPJ Web Conf. **108**, 01004 (2016).

[64] M. Christandl, N. Datta, A. Ekert, and A. J. Landahl, Perfect state transfer in quantum spin networks, Phys. Rev. Lett. **92**, 187902 (2004).

[65] P. Karbach and J. Stolze, Spin chains as perfect quantum state mirrors, Phys. Rev. A **72**, 030301(R) (2005).

[66] T. Shi, Y. Li, Z. Song, and C.-P. Sun, Quantum-state transfer via the ferromagnetic chain in a spatially modulated field, Phys. Rev. A **71**, 032309 (2005).

[67] L. Campos Venuti, C. Degli Esposti Boschi, and M. Roncaglia, Qubit teleportation and transfer across antiferromagnetic spin chains, Phys. Rev. Lett. **99**, 060401 (2007).

[68] G. M. Nikolopoulos, D. Petrosyan, and P. Lambropoulos, Electron wavepacket propagation in a chain of coupled quantum dots, J. Phys.: Condens. Matter **16**, 4991 (2004).

[69] F. Faria, C. Nelmes, T. Apollaro, T. Spiller, and I. D'Amico, Fast and efficient long-distance quantum state transfer in long-range spin-$\frac{1}{2}$ models, New J. Phys. **27**, 124503 (2025).

[70] M. Rigol, V. Dunjko, V. Yurovsky, and M. Olshanii, Relaxation in a completely integrable many-body quantum system: An *ab initio* study of the dynamics of the highly excited states of 1D lattice hard-core bosons, Phys. Rev. Lett. **98**, 050405 (2007).

[71] C. Gogolin, M. P. Müller, and J. Eisert, Absence of thermalization in nonintegrable systems, Phys. Rev. Lett. **106**, 040401 (2011).

[72] J.-S. Caux and F. H. L. Essler, Time evolution of local observables after quenching to an integrable model, Phys. Rev. Lett. **110**, 257203 (2013).

[73] A. Cantoni and P. Butler, Eigenvalues and eigenvectors of symmetric centrosymmetric matrices, Lin. Alg. Appl. **13**, 275 (1976).

[74] A. Pandey, A. Kumar, and S. Puri, Quantum chaotic systems and random matrix theory, arXiv:1905.10596v1.

[75] M. L. Mehta, *Random Matrices*, Pure and Applied Mathematics (Elsevier Science, 2004).

[76] L. F. Santos and M. Rigol, Localization and the effects of symmetries in the thermalization properties of one-dimensional quantum systems, Phys. Rev. E **82**, 031130 (2010).

[77] E. Bogomolny, U. Gerland, and C. Schmit, Short-range plasma model for intermediate spectral statistics, Eur. Phys. J. B **19**, 121 (2001).

[78] T. Guhr, A. Müller–Groeling, and H. A. Weidenmüller, Random-matrix theories in quantum physics: Common concepts, Phys. Rep. **299**, 189 (1998).

[79] W. Buijsman, V. Cheianov, and V. Gritsev, Sensitivity of the spectral form factor to short-range level statistics, Phys. Rev. E **102**, 042216 (2020).

[80] M. Schiulaz, E. J. Torres-Herrera, and L. F. Santos, Thouless and relaxation time scales in many-body quantum systems, Phys. Rev. B **99**, 174313 (2019).

[81] A. K. Das, A. Ghosh, and L. F. Santos, Spectral form factor and energy correlations in banded random matrices, Phys. Rev. B **111**, 224202 (2025).

[82] S. Seth, A. K. Das, and A. Ghosh, Signatures of nonergodicity in sparse random matrices, arXiv:2603.21369

[83] A. Ourjoumtsev, R. Tualle-Brouri, J. Laurat, and P. Grangier, Generating optical Schrödinger kittens for quantum information processing, Science **312**, 83 (2006).

[84] Y. P. Huang and M. G. Moore, Creation, detection, and decoherence of macroscopic quantum superposition states in double-well Bose-Einstein condensates, Phys. Rev. A **73**, 023606 (2006).

[85] C. Wang, Y. Y. Gao, P. Reinhold, R. W. Heeres, N. Ofek, K. Chou, C. Axline, M. Reagor, J. Blumoff, K. M. Sliwa, L. Frunzio, S. M. Girvin, L. Jiang, M. Mirrahimi, M. H. Devoret,

and R. J. Schoelkopf, A Schrödinger cat living in two boxes, Science **352**, 1087 (2016).

[86] M. Lewenstein, M. F. Ciappina, E. Pisanty, J. Rivera-Dean, P. Stammer, T. Lamprou, and P. Tzallas, Generation of optical Schrödinger cat states in intense laser–matter interactions, Nat. Phys. **17**, 1104 (2021).

[87] M. Távora, E. J. Torres-Herrera, and L. F. Santos, Inevitable power-law behavior of isolated many-body quantum systems and how it anticipates thermalization, Phys. Rev. A **94**, 041603(R) (2016).

[88] A. Jana, V. R. Chandra, and A. Garg, Local density of states and scattering rates across the many-body localization transition, Phys. Rev. B **104**, L140201 (2021).

[89] J. Louis, Correlation of local densities of states on mesoscopic energy scales in random band matrices, Lett. Math. Phys. **113**, 79 (2023).

[90] Y. Prasad and A. Garg, Single-particle excitations across the localization and many-body localization transition in quasiperiodic systems, Phys. Rev. B **109**, 094204 (2024).

[91] E. J. Torres-Herrera, A. M. García-García, and L. F. Santos, Generic dynamical features of quenched interacting quantum systems: Survival probability, density imbalance, and out-of-time-ordered correlator, Phys. Rev. B **97**, 060303(R) (2018).

[92] E. J. Torres-Herrera, J. A. Méndez-Bermúdez, and L. F. Santos, Level repulsion and dynamics in the finite one-dimensional Anderson model, Phys. Rev. E **100**, 022142 (2019).

[93] A. K. Das, C. Cianci, D. G. A. Cabral, D. A. Zarate-Herrada, P. Pinney, S. Pilatowsky-Cameo, A. S. Matsoukas-Roubeas, V. S. Batista, A. del Campo, E. J. Torres-Herrera, and L. F. Santos, Proposal for many-body quantum chaos detection, Phys. Rev. Res. **7**, 013181 (2025).

[94] I. Vallejo-Fabila, A. K. Das, D. A. Zarate-Herrada, A. S. Matsoukas-Roubeas, E. J. Torres-Herrera, and L. F. Santos, Reducing dynamical fluctuations and enforcing self-averaging by opening many-body quantum systems, Phys. Rev. B **110**, 075138 (2024).

[95] I. Vallejo-Fabila, A. K. Das, S. Choudhury, and L. F. Santos, Single-site measurements as probes of many-body quantum chaos, Phys. Rev. E **112**, 044208 (2025).

[96] E. Bogomolny and M. Sieber, Eigenfunction distribution for the Rosenzweig-Porter model, Phys. Rev. E **98**, 032139 (2018).

[97] S. Manna, S. Roy, and G. J. Sreejith, Projected ensemble in a system with locally supported conserved charges, Phys. Rev. B **111**, 144302 (2025).

[98] C. Chiu, B. Misra, and E. Sudarshan, The time scale for the quantum Zeno paradox and proton decay, Phys. Lett. B **117**, 34 (1982).

[99] L. A. Khalfin, Contribution to the decay theory of a quasi-stationary state, Sov. Phys. JETP **6**, 1053 (1958).

[100] M. Távora, E. J. Torres-Herrera, and L. F. Santos, Power-law decay exponents: A dynamical criterion for predicting thermalization, Phys. Rev. A **95**, 013604 (2017).

[101] B. Roy, A. K. Das, A. Ghosh, and I. M. Khaymovich, Anomalous energy correlations and spectral form factor in the nonergodic phase of the β ensemble, Phys. Rev. B **112**, 094206 (2025).

[102] L. F. Cugliandolo, G. Schehr, M. Tarzia, and D. Venturelli, Multifractal phase in the weighted adjacency matrices of random Erdös-Rényi graphs, Phys. Rev. B **110**, 174202 (2024).

[103] S. Sachdev, *Quantum Phase Transitions* (Cambridge University Press, 2011).

[104] W. H. Zurek, U. Dorner, and P. Zoller, Dynamics of a quantum phase transition, Phys. Rev. Lett. **95**, 105701 (2005).

[105] A. L. Corps and A. Relaño, Dynamical and excited-state quantum phase transitions in collective systems, Phys. Rev. B **106**, 024311 (2022).

[106] A. S. Matsoukas-Roubeas, M. Beau, L. F. Santos, and A. del Campo, Unitarity breaking in self-averaging spectral form factors, Phys. Rev. A **108**, 062201 (2023).

[107] P. Bocchieri and A. Loinger, Quantum recurrence theorem, Phys. Rev. **107**, 337 (1957).

[108] L. S. Schulman, Note on the quantum recurrence theorem, Phys. Rev. A **18**, 2379 (1978).

[109] F. Haake, *Quantum Signatures of Chaos* (Springer, Berlin, Heidelberg, 2010), pp. 1–14.

[110] J. H. Eberly, N. B. Narozhny, and J. J. Sanchez-Mondragon, Periodic spontaneous collapse and revival in a simple quantum model, Phys. Rev. Lett. **44**, 1323 (1980).

[111] Z. D. Gaeta and C. R. Stroud, Classical and quantum-mechanical dynamics of a quasiclassical state of the hydrogen atom, Phys. Rev. A **42**, 6308 (1990).

[112] P. Reimann, Foundation of statistical mechanics under experimentally realistic conditions, Phys. Rev. Lett. **101**, 190403 (2008).

[113] J. Gemmer and G. Mahler, Distribution of local entropy in the Hilbert space of bi-partite quantum systems: Origin of Jaynes' principle, Eur. Phys. J. B **31**, 249 (2003).

[114] M. Cramer, C. M. Dawson, J. Eisert, and T. J. Osborne, Exact relaxation in a class of nonequilibrium quantum lattice systems, Phys. Rev. Lett. **100**, 030602 (2008).

[115] M. Cramer and J. Eisert, A quantum central limit theorem for non-equilibrium systems: Exact local relaxation of correlated states, New J. Phys. **12**, 055020 (2010).

[116] A. C. Cassidy, C. W. Clark, and M. Rigol, Generalized thermalization in an integrable lattice system, Phys. Rev. Lett. **106**, 140405 (2011).

[117] L. A. Bunimovich, On the ergodic properties of nowhere dispersing billiards, Commun. Math. Phys. **65**, 295 (1979).

[118] N. Simányi, Proof of the ergodic hypothesis for typical hard ball systems, *Annales Henri Poincaré* (Springer, 2004), Vol. 5, pp. 203–233.

[119] N. Simányi, Conditional proof of the Boltzmann-Sinai ergodic hypothesis, Invent. Math. **177**, 381 (2009).

[120] H. Tasaki, From quantum dynamics to the canonical distribution: General picture and a rigorous example, Phys. Rev. Lett. **80**, 1373 (1998).

[121] S. Popescu, A. J. Short, and A. Winter, Entanglement and the foundations of statistical mechanics, Nat. Phys. **2**, 754 (2006).

[122] S. Goldstein, J. L. Lebowitz, R. Tumulka, and N. Zanghì, Canonical typicality, Phys. Rev. Lett. **96**, 050403 (2006).

[123] N. Linden, S. Popescu, A. J. Short, and A. Winter, Quantum mechanical evolution towards thermal equilibrium, Phys. Rev. E **79**, 061103 (2009).

[124] M. P. Müller, E. Adlam, L. Masanes, and N. Wiebe, Thermalization and canonical typicality in translation-invariant

quantum lattice systems, Commun. Math. Phys. **340**, 499 (2015).
[125] M. Feingold, N. Moiseyev, and A. Peres, Classical limit of quantum chaos, Chem. Phys. Lett. **117**, 344 (1985).
[126] M. Feingold and A. Peres, Distribution of matrix elements of chaotic systems, Phys. Rev. A **34**, 591 (1986).
[127] M. Lax, Relation between canonical and microcanonical ensembles, Phys. Rev. **97**, 1419 (1955).
[128] L. D'Alessio, Y. Kafri, A. Polkovnikov, and M. Rigol, From quantum chaos and eigenstate thermalization to statistical mechanics and thermodynamics, Adv. Phys. **65**, 239 (2016).
[129] G. Mussardo, Infinite-time average of local fields in an integrable quantum field theory after a quantum quench, Phys. Rev. Lett. **111**, 100401 (2013).
[130] P. Calabrese, F. H. L. Essler, and M. Fagotti, Quantum quench in the transverse-field Ising chain, Phys. Rev. Lett. **106**, 227203 (2011).
[131] F. H. L. Essler, S. Evangelisti, and M. Fagotti, Dynamical correlations after a quantum quench, Phys. Rev. Lett. **109**, 247206 (2012).
[132] M. Fagotti, Finite-size corrections versus relaxation after a sudden quench, Phys. Rev. B **87**, 165106 (2013).
[133] M. Fagotti and F. H. L. Essler, Reduced density matrix after a quantum quench, Phys. Rev. B **87**, 245107 (2013).
[134] M. Fagotti, M. Collura, F. H. L. Essler, and P. Calabrese, Relaxation after quantum quenches in the spin-$\frac{1}{2}$ Heisenberg XXZ chain, Phys. Rev. B **89**, 125101 (2014).
[135] M. Mierzejewski, P. Prelovšek, and T. Prosen, Breakdown of the generalized Gibbs ensemble for current-generating quenches, Phys. Rev. Lett. **113**, 020602 (2014).
[136] B. Pozsgay, M. Mestyán, M. A. Werner, M. Kormos, G. Zaránd, and G. Takács, Correlations after quantum quenches in the XXZ spin chain: Failure of the generalized Gibbs ensemble, Phys. Rev. Lett. **113**, 117203 (2014).
[137] E. Ilievski, J. De Nardis, B. Wouters, J.-S. Caux, F. H. L. Essler, and T. Prosen, Complete generalized Gibbs ensembles in an interacting theory, Phys. Rev. Lett. **115**, 157201 (2015).
[138] C. Gramsch and M. Rigol, Quenches in a quasidisordered integrable lattice system: Dynamics and statistical description of observables after relaxation, Phys. Rev. A **86**, 053615 (2012).
[139] T. M. Wright, M. Rigol, M. J. Davis, and K. V. Kheruntsyan, Nonequilibrium dynamics of one-dimensional hard-core anyons following a quench: Complete relaxation of one-body observables, Phys. Rev. Lett. **113**, 050601 (2014).
[140] P. Calabrese and J. Cardy, Quantum quenches in extended systems, J. Stat. Mech. (2007) P06008.
[141] D. Fioretto and G. Mussardo, Quantum quenches in integrable field theories, New J. Phys. **12**, 055015 (2010).
[142] J. Cardy, Quantum quenches to a critical point in one dimension: some further results, J. Stat. Mech. (2016) 023103.
[143] M. Rigol, V. Dunjko, and M. Olshanii, Thermalization and its mechanism for generic isolated quantum systems, Nature (London) **452**, 854 (2008).
[144] M. Ippoliti and W. W. Ho, Solvable model of deep thermalization with distinct design times, Quantum **6**, 886 (2022).
[145] A. Sherry and S. Roy, Do mixed states exhibit deep thermalisation? arXiv:2507.14135.
[146] https://github.com/AdwayDas/Symmetric_centrosymmetric_data.
[147] J. von Neumann, Proof of the ergodic theorem and the h-theorem in quantum mechanics, Eur. Phys. J. H **35**, 201 (2010).
[148] S. Goldstein, J. L. Lebowitz, C. Mastrodonato, R. Tumulka, and N. Zanghì, Normal typicality and von Neumann's quantum ergodic theorem, Proc. R. Soc. A: Math. Phys. Eng. Sci. **466**, 3203 (2010).